J. Fluid Mech. (1995), vol. 299, pp. 217–239

Drift velocity of spatially decaying waves in a two-layer viscous system

By ISMAEL PIEDRA-CUEVA†

Laboratoire des Ecoulements Géophysiques et Industriels, Institut de Mécanique de Grenoble; BP 53, 38041 Grenoble Cedex 9, France

(Received 26 July 1994 and in revised form 28 April 1995)

This paper analyses the mass transport velocity in a two-layer system induced by the action of progressive waves. First the movement inside the two layers is obtained. Next the mass transport of spatially decaying waves is calculated by solving the momentum and mass conservation equations in the Lagrangian coordinate system. Two different physical situations are analysed: the first is waves in a closed channel and the second is waves in an unbounded domain, where the steady-state mass flux may be non-zero. The influence of the viscous properties of the lower layer on the mass transport in both layers is studied. Comparison with the experiments of Sakakiyama & Bijker (1989) in a water–mud system shows good agreement. The results show that the mass transport velocity can be quite different from the velocity given by the rigid bed theory, depending on the physical properties of the lower layer.

1. Introduction

Mass transport is a steady Lagrangian current generated by wave motion. This steady flow, although small in magnitude, is important in determining the migration of sediment near the sea bed and of pollutant in a water column.

The physics of the generation of mass transport under a two-dimensional wave field is fairly well understood. If it happens that the horizontal and vertical velocity components oscillate with a phase difference other than $\pi/2$, so that the time average of their product is non-zero, there will be a net transfer of x-momentum across a surface element with normal in the z-direction. As a result of the increase of the velocity with distance from the boundary, this effective stress will vary across the boundary layer and it will thus produce a non-zero average force on the fluid (Batchelor 1967). Moreover, the residual vorticity generated inside the viscous boundary layers is diffused into the water column in the core region and also advected by the mean velocity.

Mei (1989) has shown that in the unusual situation where the wave amplitude H_s is much smaller than the Stokes boundary layer thickness $(2\nu/\sigma)^{1/2}$, where ν is the kinematic viscosity and σ the wave frequency, diffusion dominates and convection is negligible. Hence the problem is linearized and the analytical conduction solution of Longuet-Higgins (1953) is obtained. In more practical situations, the wave amplitude is greater than the boundary layer thickness and so both convection and diffusion are important. As was stated by Iskandarani & Liu (1991), in this case numerical

† Permanent address: Institute of Fluid Mechanics and Environmental Engineering (IMFIA), Faculty of Engineering. C.C. 30, Montevideo, Uruguay.

solutions are usually required. However, as will be shown later, an alternative to taking into account both convection and diffusion in an analytical approach is to employ Lagrangian coordinates.

Migniot (1968) first analysed experimentally the interface mass transport velocity induced by wave action on a two-layer system (water and mud). Dore (1970), studied this problem theoretically and concluded that the interface mass transport velocity can formally be an order of magnitude larger than that obtained by Longuet-Higgins (1953) for a single homogeneous fluid. In addition, he found that the profile of the mass transport velocity in either fluid was independent of the wavelength.

Tsuruya, Nakano & Takahama (1987) and Shibayama, Takikawa & Horikawa (1986) applied the solution of Dalrymple & Liu (1978) to study mass transport in a two-layer system, but these authors did not consider the Stokes drift investigated by Longuet-Higgins (1953) and so the mechanism of the mass transport was not fully described. Sakakiyama & Bijker (1989) have obtained the mass transport velocity inside the lower layer (mud layer) also by using the theory of Dalrymple & Liu (1978) for the first-order solution, but in that paper the second-order time-averaged horizontal pressure gradient was neglected, which precludes the existence of any second-order set-up. All the above theories were based on the Eulerian coordinate system.

Swan & Sleath (1990) pointed out that in order to obtain a solution for the flow in the boundary layer, it is desirable to adopt curvilinear coordinates, since as was shown by Longuet-Higgins, the use of Cartesian coordinates coupled with a Taylor expansion about the mean level produces a solution that is valid only for waves of extremely small amplitude. For water wave studies, the alternative to using the Lagrangian description has been explored by Pierson (1962), Chang (1969), Ünlüata & Mei (1970) and Huang (1970). More recently, Grimshaw (1981) has studied mass transport using the generalized Lagrangian-mean formulation of Andrews & McIntyre (1978).

The aim of this paper is to investigate the mass transport velocity induced by the action of decaying progressive waves propagating in a two-layer viscous system. Lagrangian coordinates are employed *a priori*, since it seems more natural in order to obtain a Lagrangian velocity. The amplitude of the surface wave is allowed to decay spatially along the channel length (x-direction) with an attenuation length scale k_j^{-1}. The upper and lower layers are modelled as viscous fluids and the mass transport in both layers is determined.

In §2 we formulate the general equations, and in §3 the equations in the Lagrangian coordinate system are derived, which will enable us to take into account both convection and diffusion of the mean vorticity from boundaries. The first-order solution for both layers is obtained in §4, and in §5 we derive the second-order solution. Finally, in §6 we apply the second-order solution to a two layer viscous system. We concentrate on two different physical situations: the first is waves in closed channels, where it is appropiate to impose a condition of zero net mass flux when calculating the mass transport velocity; and the second is waves in an unbounded domain, where the steady-state mass flux and the set-up of both the free surface and upper–lower layer interface may be non-zero.

2. Formulation

Cartesian coordinates (x, z) are introduced so that the origin is at the undisturbed interface between the two layers, z is positive upwards and the x-coordinate is positive

in the direction of wave propagation. Subscripts w and m refer to the upper and lower layer. The system is forced by a small-amplitude surface wave of frequency σ propagating in an upper layer of depth h_1 and density ρ_w and over a denser layer of depth h_2 and density ρ_m.

The equation of motion for a viscous incompressible fluid is the Navier–Stokes equation:

$$\rho \ddot{\boldsymbol{q}} = -\nabla P + \mu \nabla^2 \dot{\boldsymbol{q}} - \rho \boldsymbol{g}, \tag{2.1}$$

and the continuity equation:

$$\nabla \cdot \dot{\boldsymbol{q}} = 0, \tag{2.2}$$

where $\boldsymbol{q}$, P, μ, ρ and g denote respectively the vector fluid particle displacement with horizontal and vertical components (x, z), pressure, dynamic viscosity, fluid density and gravitational acceleration, and the overdot means time derivative.

3. Lagrangian equations

Lagrangian coordinates specify the velocity of a fluid element while it flows. In a sense, using the Lagrangian description is somewhat analogous to the coordinate transformation – in which the free surface is made a coordinate curve – used by Longuet-Higgins (1953), Dore (1973) and Craik (1982). However, mass transport is a Lagrangian quantity, and should then be more directly obtained from the corresponding formulation.

The method of analysis involves an expansion in powers of a small parameter ϵ associated with the wave amplitude and the wavelength. To simplify the perturbation form of the resulting equations and following Pierson (1962), the tags for the fluid particles will be identified by their coordinate (α,δ) either at zero time or in the undisturbed position, and (x, z) are their coordinates at any time $t \geqslant 0$. The coordinate origin being located at the interface between the two layers, the positions of the free surface, of the upper–lower layer interface and of the rigid bottom are defined by $\delta = h_1$, $\delta = 0$ and $\delta = -h_2$. Figure 1 shows a general sketch, where X_o defines the particle position at zero time, i.e. $X_o = (\alpha, \delta)$, and X defines its position at any time by the coordinates (x, z).

In this way $X = X(X_o, t)$ and $X_o = X(X_o, 0)$, and the domain of definition is given by

$$0 \leqslant \alpha \leqslant +\infty, \quad -h_2 \leqslant \delta \leqslant h_1, \quad t \geqslant 0. \tag{3.1}$$

If it is assumed that the functions $x = x(\alpha, \delta, t)$ and $z = z(\alpha, \delta, t)$ can be inverted, it is possible to express α and δ in terms of x and z, where $\alpha = \alpha(x, z, t)$ and $\delta = \delta(x, z, t)$. For a given function $f(x, z, t)$, we can obtain the components of the gradient $(\partial f/\partial x, \partial f/\partial z)$ in Eulerian coordinates by considering α and δ as two parameters:

$$\frac{\partial f}{\partial x} = \frac{\partial(f,z)}{\partial(\alpha,\delta)} \Big/ \frac{\partial(x,z)}{\partial(\alpha,\delta)}, \quad \frac{\partial f}{\partial z} = \frac{\partial(x,f)}{\partial(\alpha,\delta)} \Big/ \frac{\partial(x,z)}{\partial(\alpha,\delta)}, \tag{3.2}$$

where

$$\frac{\partial(f,z)}{\partial(\alpha,\delta)} = \begin{vmatrix} f_\alpha & f_\delta \\ z_\alpha & z_\delta \end{vmatrix} = f_\alpha z_\delta - f_\delta z_\alpha,$$

and the subindices α, δ mean $\partial/\partial\alpha$ and $\partial/\partial\delta$.

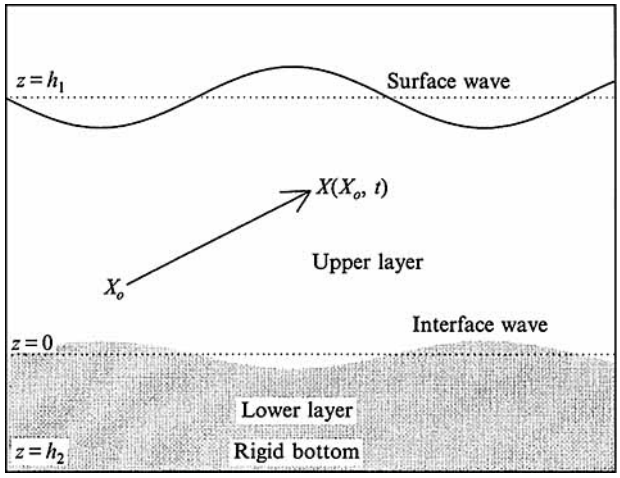

FIGURE 1. General sketch.

Applying (3.2) to (2.1) and (2.2), the mass conservation equation

$$\frac{\partial(x,z)}{\partial(\alpha,\delta)} = x_\alpha z_\delta - x_\delta z_\alpha = 1, \tag{3.3}$$

and the x- and z-momentum equations in Lagrangian form are obtained:

$$\begin{aligned}\ddot{x} = &-(1/\rho)(P_\alpha z_\delta - P_\delta z_\alpha) + \nu[z_\delta(\dot{x}_\alpha z_\delta - \dot{x}_\delta z_\alpha)_\alpha \\ &-z_\alpha(\dot{x}_\alpha z_\delta - \dot{x}_\delta z_\alpha)_\delta + x_\delta(\dot{x}_\alpha x_\delta - \dot{x}_\delta x_\alpha)_\alpha - x_\alpha(\dot{x}_\alpha x_\delta - \dot{x}_\delta x_\alpha)_\delta],\end{aligned} \tag{3.4}$$

$$\begin{aligned}\ddot{z} + g = &-(1/\rho)(P_\delta x_\alpha - P_\alpha x_\delta) + \nu[z_\delta(\dot{z}_\alpha z_\delta - \dot{z}_\delta z_\alpha)_\alpha \\ &-z_\alpha(\dot{z}_\alpha z_\delta - \dot{z}_\delta z_\alpha)_\delta + x_\delta(\dot{z}_\alpha x_\delta - \dot{z}_\delta x_\alpha)_\alpha - x_\alpha(\dot{z}_\alpha x_\delta - \dot{z}_\delta x_\alpha)_\delta].\end{aligned} \tag{3.5}$$

Equations (3.3), (3.4) and (3.5) should be solved with the proper boundary conditions. The boundary conditions are prescribed on the free surface $\delta = h_1$, where the stress is zero and the kinematic condition holds, at the interface $\delta = 0$, where there is continuity of velocity and stress, and finally at the rigid bottom $\delta = -h_2$, where there is no motion.

The stress tensor $\boldsymbol{T}$ is stated as: $\boldsymbol{T} = -P\boldsymbol{I} + \boldsymbol{\tau}$, where $\boldsymbol{I}$ is the unit tensor and $\boldsymbol{\tau}$ is related to the symmetric part of the velocity gradient tensor $\boldsymbol{D}$, being equal to $2\,\mu\boldsymbol{D}$. The tangential and normal components of the stress are obtained considering the tangential and normal vectors to the material curve $\boldsymbol{t} = (x_\alpha, z_\alpha)$ and $\boldsymbol{n} = (-z_\alpha, x_\alpha)$:

$$(\boldsymbol{Tn})\boldsymbol{t} = \frac{(\tau_{zz} - \tau_{xx})x_\alpha z_\alpha + \tau_{xz}(x_\alpha^2 - z_\alpha^2)}{\|N\|^2}, \tag{3.6a}$$

$$(\boldsymbol{Tn})\boldsymbol{n} = \frac{\tau_{zz}x_\alpha^2 + \tau_{xx}z_\alpha^2 - 2\tau_{xz}x_\alpha z_\alpha - P(x_\alpha^2 + z_\alpha^2)}{\|N\|^2}, \tag{3.6b}$$

where $\|\boldsymbol{N}\|$ is the magnitude of the vector normal to the surface. The components $(\tau_{zz}, \tau_{xx}, \tau_{xz})$ of the tensor $\boldsymbol{\tau}$ are

$$\tau_{zz} = 2\mu\frac{\partial \dot{z}}{\partial z} = 2\mu(x_\alpha \dot{z}_\delta - x_\delta \dot{z}_\alpha), \tag{3.7a}$$

$$\tau_{xx} = 2\mu\frac{\partial \dot{x}}{\partial x} = 2\mu(\dot{x}_\alpha z_\delta - \dot{x}_\delta z_\alpha), \tag{3.7b}$$

$$\tau_{xz} = \mu\left(\frac{\partial \dot{x}}{\partial z} + \frac{\partial \dot{z}}{\partial x}\right) = \mu(x_\alpha \dot{x}_\delta - x_\delta \dot{x}_\alpha + \dot{z}_\alpha z_\delta - \dot{z}_\delta z_\alpha). \tag{3.7c}$$

Following Pierson, we assume a perturbation about $x = \alpha$, $z = \delta$ and $P = P_o - \rho g\delta$ of the form

$$\boldsymbol{q} = \boldsymbol{q}_o + \epsilon \boldsymbol{q}^{(1)} + \epsilon^{(2)} \boldsymbol{q}^{(2)} + \cdots, \tag{3.8a}$$

$$P = (P_o - \rho g\delta) + \epsilon p^{(1)} + \epsilon^{(2)} p^{(2)} + \cdots, \tag{3.8b}$$

where $\boldsymbol{q}_o = (\alpha, \delta)$, $\boldsymbol{q}^{(1)} = (x^{(1)}, z^{(1)})$, $\boldsymbol{q}^{(2)} = (x^{(2)}, z^{(2)})$ and ϵ is the ordering parameter.

Note the implicit assumption made in the above perturbation expansion that the Lagrangian deformations are small.

4. First-order solution

When these perturbations are substituted into the above equations of motion and mass conservation, and when terms in the first power of ϵ are collected, the first-order equation is obtained:

$$\ddot{x}^{(1)} + g z_\alpha^{(1)} = -p_\alpha^{(1)}/\rho + \nu(\dot{x}_{\alpha\alpha}^{(1)} + \dot{x}_{\delta\delta}^{(1)}), \tag{4.1a}$$

$$\ddot{z}^{(1)} + g z_\delta^{(1)} = -p_\delta^{(1)}/\rho + \nu(\dot{z}_{\alpha\alpha}^{(1)} + \dot{z}_{\delta\delta}^{(1)}), \tag{4.1b}$$

$$\dot{x}_\alpha^{(1)} + \dot{z}_\delta^{(1)} = 0. \tag{4.1c}$$

We look for solutions for pressures and displacements of the following complex form:

$$[\boldsymbol{q}^{(1)}, p^{(1)}] = [\hat{\boldsymbol{q}}(\delta), \hat{p}(\delta)]\, \mathrm{e}^{\mathrm{i}(k\alpha - \sigma t)}, \tag{4.2}$$

where $\mathrm{i} = (-1)^{1/2}$ and the functions with a circumflex are in general complex. Only the real part of this expression should be taken.

The elevation of the free surface is defined as $\eta = H_s/2\, \mathrm{e}^{\mathrm{i}(k\alpha - \sigma t)}$, where H_s is real and k is complex, the real part of k is the wavenumber and the complex part k_j is the damping coefficient of the wave height.

Substitution of the perturbation series (3.8) into (3.6), and use of (4.2), yield for the first-order components of the stress

$$(\boldsymbol{Tn})\boldsymbol{t}^{(1)} = \rho \nu_r(\dot{x}_\delta^{(1)} + \dot{z}_\alpha^{(1)}), \tag{4.3a}$$

$$(\boldsymbol{Tn})\boldsymbol{n}^{(0)} = -(P_o - \rho_r g\delta), \tag{4.3b}$$

$$(\boldsymbol{Tn})\boldsymbol{n}^{(1)} = -(P_o - \rho_r g\delta)2x_\delta^{(1)} - p^{(1)} + 2\rho_r \nu_r \dot{z}_\delta^{(1)}, \tag{4.3c}$$

and substituting into (4.1) and solving for $p^{(1)}$ and $x^{(1)}$, the governing differential equation for $z^{(1)}$ valid for both layers is obtained:

$$z_{\delta\delta\delta\delta}^{(1)} - z_{\delta\delta}^{(1)}(l_r^2 + k^2) + z^{(1)}\, l_r^2\, k^2 = 0, \tag{4.4}$$

where

$$l_r^2 = k^2 - \mathrm{i}\sigma/\nu_r, \tag{4.5}$$

and the subindices $r = \{w, m\}$ identify the upper and lower layer.

The solution assumed here for the upper layer is

$$\hat{x}_w = \mathrm{i} m_w[W_1 \mathrm{e}^{l_w c_w} - W_2 \mathrm{e}^{-l_w \delta}] + \mathrm{i}[W_3 \sinh kc_w + W_4 \cosh kc_w], \tag{4.6a}$$

$$\hat{z}_w = W_1 \mathrm{e}^{l_w c_w} + W_2 \mathrm{e}^{-l_w \delta} + W_3 \cosh kc_w + W_4 \sinh kc_w, \tag{4.6b}$$

where $c_w = \delta - h_1$ and for the lower layer that satisfies the bottom boundary conditions

at $\delta = -h_2$:

$$\hat{x}_m = \mathrm{i}M_3[-m_m \sinh l_m c_m + \sinh kc_m] + \mathrm{i}M_4[-\cosh l_m c_m + \cosh kc_m], \quad (4.7a)$$

$$\hat{z}_m = M_3[-\cosh l_m c_m + \cosh kc_m] + M_4\left[-\frac{\sinh l_m c_m}{m_m} + \sinh kc_m\right], \quad (4.7b)$$

where $m_r = l_r/k$ and $c_m = \delta + h_2$.

It should be noted that the solutions for the upper and lower layers are slightly different. The properties of the upper layer will be considered to be of the same order as those of the water, i.e. $\rho_w = 1000\ \mathrm{Kg\ m^{-3}}$ and $\nu_w = 10^{-6}\ \mathrm{m^2\,s^{-1}}$, and the properties of the lower layer will be those of a highly viscous fluid. Following Hunt (1964), defining the non-dimensional parameters:

$$K = kh, \quad L = l_w h, \quad \beta_1 = \left(\frac{4\nu_w^2 k^3}{g}\right)^{1/4}, \quad \beta_2 = \frac{\sigma}{(gk)^{1/2}}, \quad (4.8)$$

the equation (4.5) for the upper layer becomes

$$\mathrm{i}\beta_1^2 (L^2 - K^2) = 2K^2 \beta_2. \quad (4.9)$$

In liquids of vanishing viscosity, as $\beta_1 \to 0$, K and β_2 assume their inviscid significance and remain finite. Consequently from (4.9), as $\beta_1 \to 0$, $L \to \infty$ as β_1^{-1}. Thus the presence of terms of the type $\{\cosh l_w h_1, \sinh l_w h_1\}$ indicates a singularity at $\nu_w = 0$, which precludes the use of the same solution for both layers. To tackle this problem we consider only exponential terms that vanish far from the boundaries for the upper layer.

Applying the boundary conditions of zero stress and the kinematic condition at the free surface $\delta = h_1$, the continuity of velocity and shear stress on the interface $\delta = 0$ and using (4.3), the unknown complex constants $M_3, M_4, W_1 - W_4$ are obtained:

$$\frac{M_4}{m_m}[(m_m^2 - 1)m_w R(Sl_m Ck_2 - m_m Sk_2 Cl_m) - (-m_m Sl_m + Sk_2)L_1] + m_m Clk L_2$$
$$= Cl_m[Ck_1(W_3 L_3 + W_4 L_4) - Sk_1(W_4 L_3 + W_3 L_4)] - K_1(m_w^2 - 1)(-m_m Sl_m + Sk_2)$$
$$+ Ck_2[Ck_1(W_3 K_3 + W_4 K_2) - Sk_1(W_4 K_3 + W_3 K_2)], \quad (4.10)$$

$$M_3 = \frac{K_1 m_m (m_w^2 - 1) - M_4 L_1}{m_m L_2}, \quad W_2 = K_1 + M_3(Ck_2 K_2 - Cl_m) + M_4 K_4, \quad (4.11)$$

$$W_1 = -\frac{H_s}{m_w^2 - 1}, \quad W_3 = \frac{H_s}{2}\frac{m_w^2 + 1}{m_w^2 - 1}, \quad W_4 = \frac{H_s}{2}\left[\frac{g'}{m_w^2 + 1} + \frac{4m_w}{m_w^4 - 1}\right], \quad (4.12)$$

where constants L_1–L_4, K_1–K_4, $Sk_1, Ck_1, Sk_2, Ck_2, Sl_m, Cl_m, Clk$ and g' are listed in the Appendix.

Finally, the complex wavenumber is obtained by applying the condition of continuity of normal stress through the water–mud interface:

$$-p_w^{(1)} + 2\rho_w \nu_w \dot{z}_{w\delta}^{(1)} = -p_m^{(1)} + 2\rho_m \nu_m \dot{z}_{m\delta}^{(1)}, \quad (4.13)$$

which yields (4.14), where $\rho' = \rho_w/\rho_m$, $\nu' = \nu_w/\nu_m$ and $R = (\rho'\nu')^{-1}$,

$$\rho'\nu'[-2m_w W_2 + (m_w^2 + 1)(W_4 Ck_1 - W_3 Sk_1)] = M_3[-g'(1 - \rho')Clk$$
$$-2m_m Sl_m + Sk_2(m_m^2 + 1)] + M_4[-g'(1 - \rho')K_4 - 2Cl_m + Ck_2(m_m^2 + 1)]. \quad (4.14)$$

5. Second-order solution

At the second order, the mass conservation equation is

$$x_\alpha^{(2)} + z_\delta^{(2)} = -x_\alpha^{(1)} z_\delta^{(1)} + x_\delta^{(1)} z_\alpha^{(1)}, \tag{5.1}$$

and the α and δ momentum equations for a viscous fluid are

$$\begin{aligned} &\ddot{x}^{(2)} + g z_\alpha^{(2)} + p_\alpha^{(2)}/\rho - \nu(\dot{x}_{\alpha\alpha}^{(2)} + \dot{x}_{\delta\delta}^{(2)}) = Q_x, \\ Q_x = &-\ddot{x}^{(1)} x_\alpha^{(1)} - \ddot{z}^{(1)} z_\alpha^{(1)} + \nu\{x_\alpha^{(1)}(\dot{x}_{\alpha\alpha}^{(1)} + \dot{x}_{\delta\delta}^{(1)}) + z_\alpha^{(1)}(\dot{z}_{\alpha\alpha}^{(1)} + \dot{z}_{\delta\delta}^{(1)}) \\ &-2[x_\alpha^{(1)}\dot{x}_{\alpha\alpha}^{(1)} + z_\delta^{(1)}\dot{x}_{\delta\delta}^{(1)} + \dot{x}_{\alpha\delta}^{(1)}(z_\alpha^{(1)} + x_\delta^{(1)})] - \dot{x}_\alpha^{(1)}(x_{\alpha\alpha}^{(1)} + \dot{x}_{\delta\delta}^{(1)}) - \dot{x}_\delta^{(1)}(z_{\alpha\alpha}^{(1)} + z_{\delta\delta}^{(1)})\}, \end{aligned} \tag{5.2}$$

$$\begin{aligned} &\ddot{z}^{(2)} + g z_\delta^{(2)} + p_\delta^{(2)}/\rho - \nu(\dot{z}_{\alpha\alpha}^{(2)} + \dot{z}_{\delta\delta}^{(2)}) = Q_z, \\ Q_z = &-\ddot{x}^{(1)} x_\delta^{(1)} - \ddot{z}^{(1)} z_\delta^{(1)} + \nu\{x_\delta^{(1)}(\dot{x}_{\alpha\alpha}^{(1)} + \dot{x}_{\delta\delta}^{(1)}) + z_\delta^{(1)}(\dot{z}_{\alpha\alpha}^{(1)} + \dot{z}_{\delta\delta}^{(1)}) \\ &-2[x_\alpha^{(1)}\dot{z}_{\alpha\alpha}^{(1)} + z_\delta^{(1)}\dot{z}_{\delta\delta}^{(1)} + \dot{z}_{\alpha\delta}^{(1)}(z_\alpha^{(1)} + x_\delta^{(1)})] - \dot{z}_\alpha^{(1)}(x_{\alpha\alpha}^{(1)} + \dot{x}_{\delta\delta}^{(1)}) - \dot{z}_\delta^{(1)}(z_{\alpha\alpha}^{(1)} + z_{\delta\delta}^{(1)})\}, \end{aligned} \tag{5.3}$$

which agree exactly with those obtained by Pierson (1962).

The second-order stress components to be used in the boundary condition are

$$(\boldsymbol{Tn})\boldsymbol{t}^{(2)} = \rho\nu[\dot{x}_\delta^{(2)} + \dot{z}_\alpha^{(2)} + 3(x_\alpha^{(1)} x_\delta^{(1)} - \dot{x}_\alpha^{(1)} z_\alpha^{(1)}) - \dot{x}_\alpha^{(1)} x_\delta^{(1)} + \dot{z}_\alpha^{(1)} x_\alpha^{(1)}], \tag{5.4a}$$

$$\begin{aligned} (\boldsymbol{Tn})\boldsymbol{n}^{(2)} = &-(P_o - \rho g\delta)(z_\alpha^{(1)2} + x_\alpha^{(1)2}) - 2p^{(1)} x_\alpha^{(1)} - p^{(2)} \\ &-2\rho\nu(\dot{x}_\delta^{(1)} + \dot{z}_\alpha^{(1)}) z_\alpha^{(1)} + 4\rho\nu x_\alpha^{(1)} \dot{z}_\delta^{(1)} + 2\mu[\dot{z}_\delta^{(2)} + \dot{z}_\delta^{(1)} x_\alpha^{(1)} - x_\delta^{(1)} \dot{z}_\alpha^{(1)}]. \end{aligned} \tag{5.4b}$$

With spatial decay, the mean velocity cannot be strictly unidirectional since any x- variation in the horizontal velocity must be associated with a non-zero vertical velocity. The equations (5.2) and (5.3) can be solved exactly if a stream function is defined such that

$$\dot{x}^{(2)} = -\psi_\delta, \quad \dot{z}^{(2)} = \psi_\alpha. \tag{5.5}$$

Introducing equation (5.5) into (5.2) and (5.3), it is readily shown that ψ satisfies

$$\nabla^2(-\dot{\psi} + \nu\nabla^2\psi) = Q_{x\delta} - Q_{z\alpha} = Q. \tag{5.6}$$

The concept of the stream function in Lagrangian coordinates is essentially the same as in Eulerian coordinates. However, it should be noted that mass conservation is not fulfilled exactly by ψ. This is clear when considering the time derivative of equation (5.1), since it is an inhomogeneous equation:

$$\dot{x}_\alpha^{(2)} + \dot{z}_\delta^{(2)} = -(x_\alpha^{(1)} z_\delta^{(1)})_t + (x_\delta^{(1)} z_\alpha^{(1)})_t, \tag{5.7}$$

where the subscript t means time derivative. This fact was already observed by Miche (1944) in studies of gravity waves by means of the Lagrangian formulation. To tackle this problem, Miche evaluated the mass conservation equation to one order higher than the solution obtained. As stated by Pierson (1962) as well, the consequences of the failure to satisfy the mass conservation exactly are difficult to comment upon since most work in hydrodynamics considers this equation as one not to be trifled with. Nevertheless, in our case where we are looking for a second-order steady solution, the mass conservation is verified exactly for the time-averaged stream function $\bar{\psi}$, since the time average of the right-hand side of equation (5.7) is identically zero.

The expressions Q_x and Q_z contain zeroth-order and second-order harmonics. Thus we look for second order solutions of the form

$$\psi = \bar{\psi} + \hat{\psi}\, e^{2i(k\alpha - \sigma t)}. \tag{5.8}$$

To calculate the zeroth harmonic $\bar{\varphi}$, we take the time average of equation (5.6). In deriving this equation, we use the results

$$\overline{\mathrm{Re}(\mathscr{A})\mathrm{Re}(\mathscr{B})} = \tfrac{1}{2}\mathrm{Re}(\mathscr{A}^*\mathscr{B}) = \tfrac{1}{2}\mathrm{Re}(\mathscr{A}\mathscr{B}^*),$$

$$\overline{(\mathscr{A}\mathscr{B})_t} = \overline{\mathscr{A}_t\mathscr{B}} + \overline{\mathscr{A}\mathscr{B}_t} = 0,$$

$$\overline{(\mathscr{A}\mathscr{B})_{tt}} = \overline{\mathscr{A}_{tt}\mathscr{B}} + \overline{\mathscr{A}\mathscr{B}_{tt}} = \overline{2\mathscr{A}_{tt}\mathscr{B}},$$

$\mathscr{A}$ and $\mathscr{B}$ being any two complex quantities with angular frequency σ, the asterisk denoting a complex conjugate and the bar meaning time average.

Taking time averages of (5.6), we obtain

$$\nu\nabla^2(\nabla^2\bar{\varphi}) = \bar{Q}, \tag{5.9a}$$

$$\bar{Q} = 2\nu[\overline{2x_\alpha(\dot{x}_{\delta\delta\delta} + \dot{z}_{\alpha\alpha\alpha})} - \overline{2(x_\delta + z_\alpha)(\dot{x}_{\alpha\alpha\alpha} - \dot{z}_{\delta\delta\delta})} + \overline{3x_{\alpha\alpha}(\dot{z}_{\alpha\alpha} - \dot{z}_{\delta\delta})} + \overline{x_{\delta\delta}(\dot{z}_{\alpha\alpha} + 3\dot{z}_{\delta\delta})}]. \tag{5.9b}$$

In equation (5.9) it is assumed that the motion has been established in the entire depth (i.e. $\partial\bar{\varphi}/\partial t = 0$).

It should be noted as well, that in equation (5.9*b*) the non-viscous terms on the right hand side of equation (5.6) cancel each other, otherwise these terms will be secular when solving for the upper layer.

Also, it can be seen that in the present Lagrangian formulation, the convective terms that appear in the Eulerian formulation do not appear explicitly since they are taken fully into account implicitly in the solution. The resulting equation is exact to second order in the parameter ϵ.

For the two cases analysed in this paper, the spatial – as well as temporal – wave attenuation is not necessarily small (see Piedra-Cueva 1993); in fact typical values of k_j may reach as high as 10^{-2} to 10^{-1} m^{-1}, i.e. two orders of magnitude higher than the damping coefficient for a rigid bottom. Thus, it is not possible to suppose that the boundary conditions for the mass transport in the core region are essentially unaltered from those for unattenuated waves, as assumed by Craik (1982).

In the same way, Craik (1982) pointed out the apparent inconsistency of the classical assumtion that $\mathrm{d}\bar{u}/\mathrm{d}z \to 0$ outside the bottom boundary layer. In §4, a first-order velocity profile is derived which is valid in the entire water depth, i.e. in both the boundary layer and in the core region. This profile avoids the need to use a matching condition at the outer edge of the boundary layers. In fact, it is necessary only to impose the proper boundary conditions at the interfaces and at the rigid bottom, which are well known. To second order they are: zero normal and shear stresses at the free surface; continuity of velocity and shear stress at the two-layer interface; and finally zero velocity at the bottom.

To calculate the time average of Q, i.e. $\bar{Q}$, in (5.9), the first-order displacements given by equations (4.6) and (4.7) are written in the following different way:

$$\hat{x}_r = \sum_{n_r} A_{n_r}\,\mathrm{e}^{n_r c_r}, \quad \hat{z}_r = \sum_{n_r} B_{n_r}\,\mathrm{e}^{n_r c_r}, \quad n_r = l_r, -l_r, k, -k, \tag{5.10}$$

where subindex $r = \{w, m\}$ refers to the upper and lower layer respectively, $c_w = \delta - h_1$ and $c_m = \delta + h_2$.

The right-hand side of (5.9) can be stated as

$$\bar{Q} = \nu_r \mathrm{e}^{-2k_j\alpha} \sum_{j_r}\sum_{n_r} \tilde{Q}_{j_r n_r}\mathrm{e}^{(j_r + n_r)c_r}, \tag{5.11a}$$

$$\tilde{Q}_{j_r n_r} = 2\sigma\{\mathrm{i}A_{j_r}B_{n_r}[k^*k^3 - j_r n_r^3 - \tfrac{3}{2}(k^2)^*(k^2 + n_r^2) + \tfrac{1}{2}j_r^2(k^2 - 3n_r^2)]$$
$$+A_{j_r}A_{n_r}(-k^*n_r^3 + j_r k^3) - B_{j_r}k^*(\mathrm{i}k^3 A_{n_r} + n_r^3 B_{n_r})\}, \tag{5.11b}$$

which is valid for both layers with the proper selection of subindex r and where $j_r = n_r^*$, $A_{j_r} = A_{n_r}^*$, etc.

Since the α dependence of $\bar{Q}$ is concentrated in the term $\mathrm{e}^{-2k_j\alpha}$, it is valid to assume that a steady-state solution $\bar{\psi}$ exists with the form

$$\bar{\psi} = \phi(\delta)\,\mathrm{e}^{-2k_j\alpha}. \tag{5.12}$$

Substituting equations (5.12) into (5.9) and using (5.11*a*), the inhomogeneous biharmonic differential equation for ϕ is obtained:

$$\phi_r^{IV} + \phi_r^{II}2a^2 + \phi_r a^4 = \sum_{j_r}\sum_{n_r}\tilde{Q}_{j_r n_r}\mathrm{e}^{(j_r+n_r)c_r}, \tag{5.13}$$

where Roman numerals mean derivatives with respect to δ and $a = 2k_j$.

The general solution of this inhomogeneous differential equation is

$$\phi_r = (A_{r2} + c_r B_{r2})\cos ac_r + (C_{r2} + c_r D_{r2})\sin ac_r + \sum_{j_r}\sum_{n_r}H_{j_r n_r}\mathrm{e}^{(j_r+n_r)c_r}, \tag{5.14a}$$

$$H_{j_r n_r} = \frac{\tilde{Q}_{j_r n_r}}{(j_r + n_r)^4 + 2a^2(j_r + n_r)^2 + a^4}, \quad (j_r + n_r) \neq \pm\mathrm{i}a. \tag{5.14b}$$

6. Waves propagating in a two-layer viscous system

Some years ago, Dore (1970) carried out a detailed study of the mass transport velocities induced by water waves in a two-layer fluid system of finite depth. Such a Lagrangian velocity was calculated using an Eulerian coordinate system. In a subsequent paper, Dore (1973), he presented an extension and reformulation of his previous paper, since the interfacial boundary conditions were satisfied only at the equilibrium level, and this is satisfactory only when the perturbation parameter based on the wave slope $\epsilon \ll Re = (\nu_w k^2/\sigma)^{1/2}$, Re^{-1} being the representative wave Reynolds number. In fact this condition is – as was stated by Dore (1970) – a severe one, so that this work can only be regarded as a preliminary analysis. In the second paper, Dore (1973) employed the orthogonal curvilinear coordinate formulation of Longuet-Higgins (1953) to the case of an interface. Dore (1973) also assumed that both the upper and lower fluids were amenable to boundary layer analysis, and therefore, the whole fluid region was divided into the boundary layer region and the core region. The necessary condition for this situation to be valid was specified by Dore (1973): it is that the boundary layer thickness in the oscillatory fluid should be much less than both the corresponding fluid depths h_1 and h_2.

In our case in which we consider the lower layer as a highly viscous fluid mud, with a kinematic viscosity ν_m between 10^{-4} and 10^{-2} m^2 s^{-1}, the ratio between the boundary layer thickness and the fluid depth $(2\nu_m/\sigma)/h_2$ is about 0.1–0.2, and thus the above condition is not completely satisfied. Instead, a fully viscous solution for the lower layer should be looked for, as is the solution presented in this paper.

As stated by Foda, Hunt & Chou (1993), at high strain amplitudes the shear modulus of muddy bottoms is negligible, and the sediment behaves as a viscous fluid characterized only by a viscosity. In general, this viscosity is a function of the shear rate and in this condition the mud may be modelled as a Bingham body, as was

done by Sakakiyama & Bijker (1989). Nevertheless in analogy with the viscosity of a Newtonian fluid, an apparent viscosity μ_a can be employed, defined as $\tau = \mu_a \mathrm{d}u/\mathrm{d}z$, which can be determined at a convenient shear rate according to the problem to be considered.

Equation (5.14) is used to describe the mass transport velocity in the two layers. The four unknown constants A_{r2}–D_{r2} are obtained by applying the boundary conditions corresponding to the physical situation considered.

6.1. *Waves in closed channels*

The four unknown constants of (5.14*a*) for each layer are obtained by applying the boundary conditions of zero tension at the free surface, continuity of velocity and stress at the two-layer interface and zero velocity at the rigid bottom. However, if the free surface set-up is non-zero, as is the case for waves in closed channels since a horizontal hydrostatic pressure gradient is established to balance the radiation stress of the progressive wave and thus to produce the inverted flow, a further boundary condition should be imposed. The additional condition usually employed is the condition of zero net mass flux at each downstream location x.

Since we are not interested primarily in calculating the free surface set-up and we work with the stream function, it is more appropiate to replace the condition of zero normal stress by the condition of zero flux, which can be easily stated as $\bar{\psi} = 0$.

We start with the boundary conditions at the free surface $c_w = 0$ or $\delta = h_1$.

(i) Zero flux, $\bar{\psi} = 0$,

$$A_{w2} = \sum_{j_w} \sum_{n_w} -H_{j_w n_w}. \tag{6.1}$$

(ii) Zero shear stress: $\overline{(\boldsymbol{Tn})\boldsymbol{t}^{(2)}} = 0$.

Taking the time average of (5.4*a*) and using the first-order velocity given by (5.10), the condition becomes

$$\overline{\dot{x}_\delta^{(2)}} + \overline{\dot{z}_\alpha^{(2)}} = 0.$$

Substituting (5.5) and (5.12)

$$-\phi_{\delta\delta} + a^2\phi = 0,$$

and using (5.14)

$$2a(aA_{w2} - D_{w2}) = \sum_{j_w} \sum_{n_w} -H_{j_w n_w}(a^2 - \Delta_w^2), \tag{6.2}$$

where $\Delta_r = (j_r + n_r)$.

Next we apply the boundary conditions at the bottom $c_m = 0$ or $\delta = -h_2$.

(iii) Zero vertical velocity $\overline{\dot{z}_m^{(2)}} = \bar{\psi}_m = 0$,

$$A_{m2} = \sum_{j_m} \sum_{n_m} -H_{j_m n_m}. \tag{6.3}$$

(iv) Zero horizontal velocity $\overline{\dot{x}_m^{(2)}} = -\bar{\psi}_{m\delta} = 0$,

$$B_{m2} = -aC_{m2} - \sum_{j_m} \sum_{n_m} H_{j_m n_m} \Delta_m. \tag{6.4}$$

Finally, we apply the boundary conditions at the two-layer interface $c_w = -h_1$ and $c_m = h_2$.

One condition is the continuity of vertical velocity $\overline{\dot{z}_w^{(2)}} = \overline{\dot{z}_m^{(2)}}$ or $\bar{\psi}_w = \bar{\psi}_m$. Under

the conditions of zero total horizontal flow in each layer, this condition becomes $\bar{\psi}_w = \bar{\psi}_m = 0$.

(v) $\bar{\psi}_m = 0$,

$$C_{m2}(\sin ah_2 - ah_2 \cos ah_2) + D_{m2}h_2 \sin ah_2 = P_{m1}. \tag{6.5}$$

(vi) $\bar{\psi}_w = 0$,

$$-h_1 \cos ah_1 B_{w2} + C_{w2} \sin ah_1 = P_{w1}, \tag{6.6}$$

where constants P_{m1}, P_{w1}, P_{21} and P_3 are given in the Appendix.

(vii) Continuity of horizontal velocity $\overline{\dot{x}_w^{(2)}} = \overline{\dot{x}_m^{(2)}}$ or $\bar{\psi}_{w\alpha} = \bar{\psi}_{m\alpha}$,

$$B_{w2}\left(\cos ah_1 - \frac{ah_1}{\sin ah_1}\right) - C_{m2}\frac{(ah_2)^2 - \sin^2 ah_2}{h_2 \sin ah_2} = P_{21}. \tag{6.7}$$

(viii) Continuity of the shear stress $\overline{(\boldsymbol{Tn})\boldsymbol{t}^{(2)}}|_w = \overline{(\boldsymbol{Tn})\boldsymbol{t}^{(2)}}|_m$.

From equation (5.4*a*), the shear stress at the interface is

$$\overline{(\boldsymbol{Tn})\boldsymbol{t}^{(2)}}|_r = \rho_r \nu_r [\overline{\dot{x}^{(2)}}_{r\delta} + \overline{\dot{z}^{(2)}}_{r\alpha} - 2\sigma k^* \hat{x}_r^*(\hat{x}_{r\alpha} + ik\hat{z}_r)],$$

or after substitution of (5.10) and (5.12):

$$\rho' \nu' [-\phi_{w\delta\delta} + a^2\phi_w - \hat{T}_w] = [-\phi_{m\delta\delta} + a^2\phi_m - \hat{T}_m], \tag{6.8a}$$

$$\hat{T}_r = \sum_{j_r}\sum_{n_r} 2\sigma k^* A_{j_r}(n_r A_{j_r} + ikB_{j_r} e^{\Delta_r c_r}). \tag{6.8b}$$

Noting that at the interface $\phi_w = \phi_m = 0$, substituting (5.14) we obtain

$$-\rho' \nu' 2a \cos ah_1 B_{w2} - C_{m2}\frac{2a(ah_2 - \cos ah_2 \sin ah_2)}{h_2 \sin ah_2} = P_3. \tag{6.9}$$

Solving for C_{m2} from (6.7) and (6.9):

$$C_{m2}\left[\frac{-\rho' \nu' \sin^2 ah_1}{-\sin ah_1 \cos ah_1 + ah_1}(a^2h_1^2 - \sin^2 ah_1) + (\cos ah_2 \sin ah_2 + ah_2)\right]$$
$$= \frac{h_2 \sin ah_2}{2a}\left[P_3 + \frac{P_{21}\, 2a\rho' \nu' \sin^2 ah_1}{-\cos ah_1 \sin ah_1 + ah_1}\right]. \tag{6.10}$$

Obtaining C_{m2} from (6.10), the other unknown constants are determined straightforwardly by substitution of C_{m2} back into (6.4)–(6.7).

6.2. *Waves in an unbounded domain*

In unbounded domains, it is reasonable to assume that both the steady mass flux and the set-up are non-zero. For waves propagating in a water layer of constant depth, the order of magnitude of the free surface set-up is $\xi_\alpha \sim H_s^2 k_j / h_1$. If the bottom is modelled as a rigid body, typical values of the wave damping coefficient k_j are of the order of 10^{-3} m^{-1} and under such conditions the set-up is negligible. But when considering waves propagating over a non-rigid bed, the damping coefficient may be two orders of magnitude higher and a set-up should therefore exist to compensate the radiation stress flux.

To solve this case, we start by applying the boundary condition of zero stress at the free surface $c_w = 0$:

(i) zero normal stress: $\overline{(\boldsymbol{Tn})\boldsymbol{n}^{(2)}} = \overline{p_w^{(2)}} = 0$.

Following Kravtchenko & Daubert (1957), to verify this condition it is enough to impose the following alternative condition:

$$\overline{p_{w\alpha}^{(2)}} = 0. \tag{6.11}$$

After averaging in time, the x-momentum equation (5.2) for the water layer becomes

$$\overline{p_{w\alpha}^{(2)}}/\rho_w + g\overline{z_{w\alpha}^{(2)}} - \nu_w \nabla^2 \overline{\dot{x}_w^{(2)}} = \bar{Q}_{wx}, \quad c_w = 0, \tag{6.12}$$

Substituting (6.11) into (6.12) and considering that at the free surface $\overline{z_w^{(2)}} = \xi_w$, we get

$$g\xi_{w\alpha} - \nu_w \nabla^2 \overline{\dot{x}_w^{(2)}} = \bar{Q}_{wx} = \bar{Q}_{wn} + \bar{Q}_{wv}, \tag{6.13}$$

where $\bar{Q}_{wn}$ and $\bar{Q}_{wv}$ are the non-viscous and viscous parts of $\bar{Q}_{xw}$ as defined in (5.2).

Since $x^{(1)} = O(H_s)$, $\dot{x}^{(2)} = O(\sigma k H_s^2)$, $\xi_{w\alpha} = O(k_j H_s^2/h_1)$, equation (6.13) can be rescaled to give the following dimensionless groups:

$$\left[\frac{g k_j h_1}{\nu_w \sigma k} \quad 1 \quad \frac{k_j h_1^2 \sigma}{\nu_w k} \quad 1\right]. \tag{6.14}$$

Under typical conditions, the order of magnitude of the two dimensionless groups of (6.14) is $10^3 - 10^4$: thus if they do not vanish they would give secular terms. Vanishing of the non-viscous terms means

$$g\xi_{w\alpha} = -(\overline{\ddot{x}^{(1)} x_\alpha^{(1)}} + \overline{\ddot{z}^{(1)} z_\alpha^{(1)}}),$$

and after the time average is taken, the free surface set-up is

$$\xi_{w\alpha} = \frac{\sigma^2}{2g} k_j e^{-2k_j\alpha} [\| \hat{x}_w \|^2 + \| \hat{z}_w \|^2], \quad c_w = 0. \tag{6.15}$$

The remaining two viscous terms of (6.13) give the following relation:

$$a^2 \phi_\delta + \phi_{\delta\delta\delta} = P_{w3},$$

$$P_{w3} = \frac{\sigma}{2} \sum_{j_w} \sum_{n_w} \left[-4k^* n_w^2 A_{j_w} A_{n_w} + (k^2 - 3n_w^2)(k^* + \frac{j_w^2}{k^*}) B_{j_w} B_{n_w} \right],$$

where $\bar{Q}_{wv} = \nu_w e^{-2k_j\alpha} P_{w3}$. Substituting (5.14) for the upper layer ($r = w$):

$$B_{w2} = \frac{-P_{w3}}{2a^2} + \sum_{j_w} \sum_{n_w} \frac{H_{j_w n_w}}{2a^2} \Delta_w (a^2 + \Delta_w^2). \tag{6.16}$$

(ii) Zero shear stress: $\overline{(\boldsymbol{T}\boldsymbol{n})\boldsymbol{t}^{(2)}} = \overline{\dot{x}_\delta^{(2)}} + \overline{\dot{z}_\alpha^{(2)}} = 0$.
This condition gives again (6.2).

The boundary conditions (iii) and (iv) at the bottom are the same as (6.3) and (6.4).

(v) At the interface, we start by imposing $\overline{\dot{z}_w^{(2)}} = \overline{\dot{z}_m^{(2)}}$, which gives

$$A_{w2}(\cos ah_1 + ah_1 \sin ah_1) - \sin ah_1 C_{w2} - C_{m2}(\sin ah_2 - ah_2 \cos ah_2) - D_{m2} h_2 \sin ah_2 = P_1, \tag{6.17}$$

where constant P_1, P_{22}, P_4 and P_5 are given in the Appendix.

(vi) Now the continuity of horizontal velocities $\overline{\dot{x}_w^{(2)}} = \overline{\dot{x}_m^{(2)}}$ gives

$$-A_{w2} a^2 h_1 \cos ah_1 + a \cos ah_1 C_{w2} - C_{m2} a^2 h_2 \sin ah_2 - D_{m2}(\sin ah_2 + ah_2 \cos ah_2) = P_{22}. \tag{6.18}$$

(vii) The continuity of shear stress can be stated as

$$(R^{-1}-1)a^2\phi_m - R^{-1}\phi_{w\delta\delta} + \phi_{m\delta\delta} = R^{-1}\hat{T}_w - \hat{T}_m,$$

where $\hat{T}_r$ is given by (6.8).

After susbstituting ϕ:

$$C_{m2}a[-(R^{-1}-2)a^2h_2\cos ah_2 + R^{-1}a\sin ah_2] + D_{m2}a[(R^{-1}-2)ah_2\sin ah_2 + 2a\cos ah_2] - R^{-1}a^2[A_{w2}(\cos ah_1 - ah_1\sin ah_1) + \sin ah_1 C_{w2}] = P_4. \quad (6.19)$$

(viii) Continuity of normal stress $\overline{(\boldsymbol{Tn})\boldsymbol{t}^{(2)}}|_w = \overline{(\boldsymbol{Tn})\boldsymbol{t}^{(2)}}|_m$, which can be stated as $\overline{p_w^{(2)}} = \overline{p_m^{(2)}}$.

As in the case of the free surface, we impose again the condition of continuity of pressure. After using the x-momentum equation (6.12) written for the upper and lower layers and considering that at the interface $\overline{z_w^{(2)}} = \overline{z_m^{(2)}} = \xi_m$, we obtain

$$g\xi_{m\alpha}(1-\rho') + \rho' v_w \nabla^2 \overline{\dot{x}_w^{(2)}} + \rho' \bar{Q}_{wn} + \rho' \bar{Q}_{wv} = v_m \nabla^2 \overline{\dot{x}_m^{(2)}} + \bar{Q}_{mn} + \bar{Q}_{mv}, \quad (6.20)$$

where again $\bar{Q}_{rn}$ and $\bar{Q}_{rv}$ are the non-viscous and viscous parts of $\bar{Q}_{xr}$ for both layers. Since now $x^{(1)} = O(H_i)$, $\dot{x}^{(2)} = O(\sigma k H_i^2)$, $\xi_{m\alpha} = O(k_j H_i^2/h_2)$, where H_i is the interfacial wave amplitude, equation (6.20) can be rescaled as well, to give the following dimensionless groups:

$$\left[\frac{(1-\rho')}{\rho'}\frac{gk_jh_1^2}{v_w\sigma kh_2} \quad 1 \quad \frac{k_jh_1^2\sigma}{v_wk} \quad 1 \quad \frac{h_1^2v_m}{h_2^2v_w\rho'} \quad \frac{k_jh_1^2\sigma}{v_wk\rho'} \quad \frac{h_1^2v_m}{h_2^2v_w\rho'}\right]. \quad (6.21)$$

Under typical conditions, the order of magnitude of all the dimensionless groups is $\gg 1$, i.e. the viscous terms of the water layer can be neglected. This means that to second order the contribution of water viscosity to the pressures is negligible. The resulting equation

$$g\xi_{m\alpha}(1-\rho') + \rho'\bar{Q}_{wn} = v_m\nabla^2\overline{\dot{x}_m^{(2)}} + \bar{Q}_{mn} + \bar{Q}_{mv}, \quad (6.22)$$

has two unknows: the interfacial set-up and the interfacial velocity, and thus another equation is needed. The set-up of the two-layer interface can be calculated aproximately by using the x-momentum equation integrated on the lower layer. This equation can be stated as:

$$U\frac{\partial U}{\partial x} + g\frac{\partial(b_w+b_m)}{\partial x} - \frac{\rho_m-\rho_w}{\rho_m}g\frac{\partial b_w}{\partial x} = -\frac{\mathscr{T}_b-\mathscr{T}_i}{\rho_m h_2} - \frac{\mathscr{S}_{xx}}{\rho_m h_2}, \quad (6.23)$$

where U is the depth-averaged second-order velocity (assumed to be time independent), $b_w = h_1 + \xi_w$ and $b_m = h_2 + \xi_m$, $\mathscr{T}_b$ and $\mathscr{T}_i$ are the second-order shear stress at the bottom and at the two-layer interface and $\mathscr{S}_{xx}$ is the x-component of the radiation stress tensor, as defined by Longuet-Higgins.

Since the drift velocity U is of order 2 in the parameter ϵ, the convective terms are of order 4 and can be neglected. Assuming that $\xi_w \ll h_1$ and $\xi_m \ll h_2$, the interface set-up can be calculated as

$$g\frac{\partial\xi_m}{\partial x} = -\rho' g\frac{\partial\xi_w}{\partial x} - \frac{\mathscr{T}_b-\mathscr{T}_i}{\rho_m h_2} - \frac{\mathscr{S}_{xx}}{\rho_m h_2}. \quad (6.24)$$

Since all the terms in equation (6.24) are of second order, it is possible to transform to Lagrangian coordinates simply by replacing the x-derivative by the α-derivative.

Run	ρ_m(Kg m^{-3})	ν_m(m^2 s^{-1})	H_s(m)
A3	1380	1.5×10^{-2}	0.038
B1	1300	1×10^{-2}	0.027
C2	1230	4×10^{-3}	0.032
D2	1140	1×10^{-3}	0.032

TABLE 1. Experimental conditions.

Introducing (6.24), written in Lagrangian coordinates into (6.22), and using (5.5) and (5.12), we obtain

$$-2a^3 \cos ah_2(2-\rho')C_{m2} + D_{m2}[2a^2 \sin ah_2\ 2/h_2 a(1-\rho')(1-\cos ah_2 + h_2 a \sin ah_2)] = P_5. \tag{6.25}$$

This set of equations allows the calculation of the eight unknown constants of equation (5.14).

6.3. *Results*

The results of the present model are compared with the experimental and numerical results of Sakakiyama & Bijker (1989). The velocities calculated by the present model were obtained for the case of an unbounded domain. The steady-state mass transport flow is reached when the flow is established throughout the length of the wave flume. This time scale is $T_L = L/\sigma k H_s^2 = O(100$ min) where L is the flume length. It is possible that the mass transport velocity after the 1–3 minutes of the test has not been completely established in the wave flume, and so the condition of an unbounded domain may be more suited to the experimental conditions.

The laboratory experiments of Sakakiyama & Bijker (1989) were performed in a wave flume 24.5 m long, 0.50 m wide and 0.57 m deep. Water was used for the upper layer and a mix of water and mud was used as the lower layer. The initial thickness of the mud layer was about 0.09 m and the water depth was fixed at 0.30 m in all the experiments. The time period in all tests employed was about 1.0 s and the duration time of wave action was about 1–3 minutes. Table 1 shows the experimental conditions.

The velocities are expressed in non-dimensional form by using the mass transport velocity at the two-layer interface (u_o) calculated numerically by Sakakiyama & Bijker (1989) as the normalization velocity. The vertical coordinates are normalized by the mud thickness h_2 in such a way that $Z = 0$ means the rigid bottom and $Z = 1$ means the two layer interface.

Figure 2 shows the comparison of the profiles of mass transport velocity in the lower layer (mud layer) measured and calculated by Sakakiyama & Bijker (1989) and calculated with the present model. It can be seen that in general there is a good agreement between the measured velocities and those calculated by the present model. For runs B1 (figure 2*b*), C2 (figure 2*c*) and D2 (figure 2*d*), the result of the present model near the water–mud interface is an improvement on that of Sakakiyama & Bijker (1989). For run A3 (figure 2*a*) , the result of Sakakiyama & Bijker (1989) is slightly better than the present one. This result could be due to the fact that run A3 corresponds to a mud density and viscosity of 1380 Kg m^{-3} and 1.5×10^{-2} m^2 s^{-1}, i.e. to the situation of a very viscous fluid with a high density. It should be noted that the model of Sakakiyama & Bijker is restricted to the lower layer and assumes that

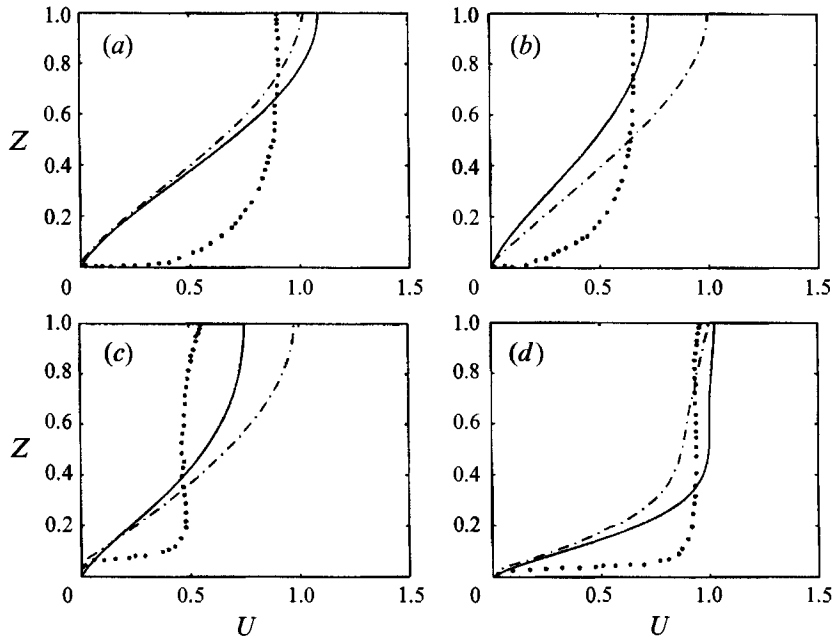

FIGURE 2. Drift velocity profile in the mud layer: •, measured (Sakakiyama & Bijker); – · –, calculated (Sakakiyama & Bijker); —, calculated (Piedra-Cueva, present model). (*a*) Run A3, $u_o = 4.9 \times 10^{-4}$ m s^{-1}, at $x = 3.5$ m; (*b*) Run B1, $u_o = 5.7 \times 10^{-4}$ m s^{-1}, at $x = 5.0$ m; (*c*) Run C2, $u_o = 1.1 \times 10^{-3}$ m s^{-1}, at $x = 6.0$ m; (*d*) Run D3, $u_o = 1.11 \times 10^{-3}$ m s^{-1}, at $x = 6.0$ m.

the second-order time-average pressure gradient is zero, which may be more suited to the actual experimental conditions.

It can be seen from figure 2, that the profiles of mass transport velocity measured by these authors are more uniform than those obtained theoretically. The greatest differences appear near the rigid bed, where both the numerical solution of Sakakiyama & Bijker and the present analytical solution give smaller velocities than the experimental results. It is thought that this effect is due to the fact that the theoretical solutions are based on Newtonian fluids, while it is well known that mud behaves as non-Newtonian fluid, i.e. the mud viscosity changes as a function of the shear rate. In fact, the viscosity decreases for increasing shear rate. Thus, mud at deeper levels moves faster than predicted, since shear rate increases near the rigid bottom and viscosity decreases.

Next, we present the profile of mass transport velocity in both the upper and lower layers as obtained with the present model, for various values of the lower-layer viscosity ν_m, which are shown in figure 3(*a–d*). Figures 3(*a*) and 3(*c*) were obtained for the case of short waves – $k_o h_1 = 1.37$ – and figures 3(*b*) and 3(*d*) for the case of long waves – $k_o h_1 = 0.57$ –, where k_o is the wavenumber given by the rigid bed theory.

In all cases, the solid lines represent the velocity profile for high values of ν_m – the viscosity of the lower layer – , i.e. the rigid bed solution. Figures 3(*a*) and 3(*b*) were calculated with the unbounded domain condition and figures 3(*c*) and 3(*d*) with the condition of zero flux. All the results presented here were obtained with a given set of fixed physical parameters, which are stated in each figure.

In the case of the unbounded domain (figures 3*a* and 3*b*), the mass transport in the upper layer decreases for decreasing viscosities of the lower layer, and is always

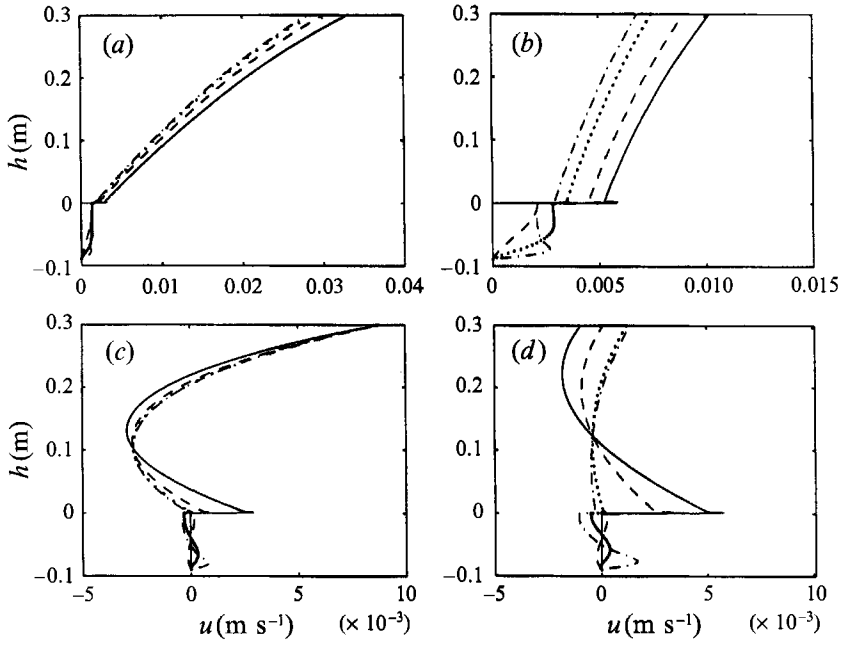

FIGURE 3. Profile of horizontal mass transport velocity for a two-layer viscous system. The characteristics of the system are: $h_1 = 0.30$ m, $h_2 = 0.09$ m, $\rho_m = 1230$ Kg m^{-3}; (*a*) and (*c*) $k_o h_1 = 1.37$, (*b*) and (*d*) $k_o h_1 = 0.57$; (*a*) and (*b*) unbounded domain, (*c*) and (*d*) zero flux: ν_m(m^2 s^{-1}) = —, 10^3; – · –, 10^{-4}; •, 10^{-3}; – –, 10^{-2}. $H_s = 0.032$ m.

smaller than that obtained for the case of a rigid bed. For the range of viscosities studied, changes of about 40% in the velocity occur. In the lower layer the velocity in general increases for decreasing viscosities, and thus the velocity jump through the interface boundary layers follows the change in viscosity. For vanishing viscosity and for $\rho_m \to \rho_w$, the velocity jump should be zero, as in the case of a one-layer system with thickness $h_1 + h_2$. The interface mass transport is always in the direction of wave propagation, from left to right in these figures.

For the range of intermediate values of $k_o h_1$ considered, it is seen that in the upper layer the velocity near the free surface decreases for decreasing $k_o h_1$, while near the interface the velocity increases, and so the resulting velocity profile is more uniform for the case of longer waves. The flow rate in the upper layer increases for increasing wave frequencies, while in the lower layer in general it decreases. We will come back to this point later on.

Figures 3(*c*) and 3(*d*) show the resulting velocity profiles for the case of waves in a closed domain. In the interior of the upper fluid, the velocity has a parabolic distribution, with positive or negative values at the free surface, depending on the wave frequency and on the viscosity of the lower-layer. While for the shorter waves ($k_o h_1 = 1.37$) the free surface velocity is always positive and almost independent of the lower layer viscosity, for the longer waves this velocity can be positive, zero or negative depending on ν_m. For this case, the rigid bed solution predicts negative velocities at the free surface, but from figure 3(*d*) it is seen that it becomes positive for decreasing ν_m. In fact, for $\nu_m = 10^{-4}$ m^2 s^{-1} the velocity profile in all the upper column is completely inverted with respect to the rigid bed solution. Also in this

case, the total horizontal flow due to the mass transport is zero, as was imposed. The interfacial velocity can take positive or negative values, depending on σ and ν_m.

The profile of mass transport velocity in the lower fluid is similar to that in the upper fluid, but now the form of the velocity profile has slightly changed in relation to that presented by Dore (1970), which is thought to be due to the use of the Lagrangian formulation. In fact, as was stated by Dore (1970, p. 123), in the Eulerian formulation the stress and the second-order Eulerian mean velocity are discontinuous across $z = 0$. They are continuous across the actual position of the interface. But this is not the case in the Lagrangian formulation, since both stress and velocity are continuous across the interface in the reference configuration, which was taken as the undisturbed position $z = 0$. The velocity profiles in this lower layer are fairly sensitive to variations in ν_m. As is seen from figures 3(*c*) and 3(*d*), changes in the wavelength modify mainly the magnitude of the velocity, but not the form of the profile.

It is interesting to note that while the formal solution of the mass transport velocity (equation (5.14)) is independent of the fluid viscosity as was obtained as well by Longuet-Higgins for the case of a homogeneous fluid, the solution is highly sensitive to the viscosity of the lower layer. This is due to the fact that viscosity effects are introduced in three differents way: through the first-order solution, through the wave damping coefficient k_j and finally through the second-order boundary conditions by which the unknown constants of (5.14) are calculated.

Next, the interfacial velocity is analysed in more detail. Figure 4(*a–d*) shows the interfacial velocity as a function of the wave frequency. Figures 4(*a*) and 4(*b*) are for various viscosity values (ν_m), and figures 4(*c*) and 4(*d*) are for various density values (ρ_m). It is seen that for both $\sigma \to \infty$ and $\sigma \to 0$ the interfacial velocity reduces to zero as should be expected, since the first case means deep water waves and the second means steady-state flow. For the larger viscosity value ($\nu_m = 10^{-2}\ \mathrm{m^2\,s^{-1}}$), the interfacial velocity has a bell shaped variation with σ, for both the bounded and unbounded cases (figures 4*a* and 4*b*). The maximum value is obtained in both cases for $\sigma \approx 3.5\ \mathrm{rad\,s^{-1}}$, and the velocity always remains positive. For the lower viscosities (ν_m between 5×10^{-4} and $10^{-3}\ \mathrm{m^2\,s^{-1}}$), in the case of an unbounded domain, the interfacial velocity increases almost linearly with decreasing frequencies up to about $\sigma = 1\ \mathrm{rad\,s^{-1}}$, and then decreases strongly towards zero for $\sigma \to 0$. The maximum velocity value now is about twice the velocity for $\nu_m = 10^{-2}\ \mathrm{m^2\,s^{-1}}$, i.e. the interfacial velocity increases for decreasing viscosities. For the case of bounded domains (figure 4*b*), it is seen that the variation of the interfacial velocity with the wave frequency is rather complex in the same range of ν_m. Interfacial velocities are negative and increase (in an absolute sense) for decreasing ν_m. Note the strong variation of the interfacial velocity that occurs for $\nu_m = 10^{-3}$–$10^{-2}\ \mathrm{m^2\,s^{-1}}$.

Figures 4(*c*) and 4(*d*) show the variation of the interface mass transport for various values of the lower-fluid density. The velocity is not too sensitive to the variation of ρ_m, but once again it changes considerably with wave frequency. It should be noted that the shape of the interfacial velocity of figure 4(*d*) ($\nu_m = 10^{-3}\ \mathrm{m^2\,s^{-1}}$) becomes very similar to the curve presented in figure 4(*c*) for $\nu_m = 4 \times 10^{-3}\ \mathrm{m^2\,s^{-1}}$, showing the importance of this parameter.

Figures 5(*a*) and 5(*b*) show the amplification factor A_f and the shift factor S_f (expressed in degrees), plotted as a function of the wave frequency and for different ν_m values. The amplification factor is defined as the ratio of the interfacial wave height to the surface wave height, and the shift factor as the relative phase angle between the interfacial wave motion and the surface wave motion. It is seen that A_f decreases for increasing ν_m, with a bell shaped variation with the wave frequency. The

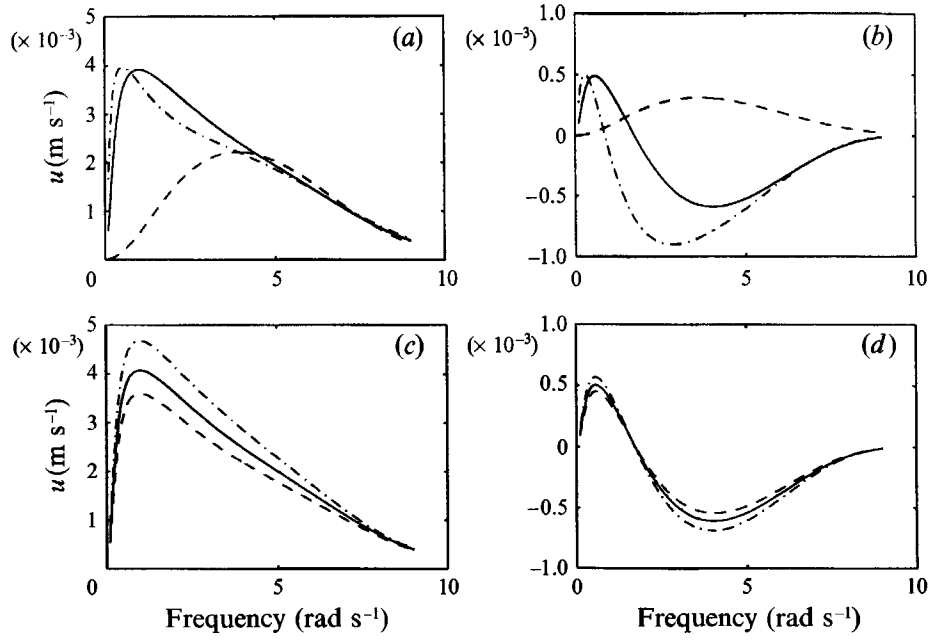

FIGURE 4. Interfacial mass transport velocity versus wave frequency for various viscosities and densities of the lower layer. $h_1 = 0.30$ m, $h_2 = 0.09$ m; (*a*) and (*c*) unbounded domain, (*b*) and (*d*) zero flux; (*a*) and (*b*): ν_m(m^2 s^{-1}) = – · –, 5×10^{-4}, —, 10^{-3}; ——, 10^{-2}, $\rho_m = 1230$ Kg m^{-3}; (*c*) and (*d*): ρ_m(Kg m^{-3}) = – · –, 1100; —, 1200; ——, 1300, $\nu_m = 10^{-3}$ m^2 s^{-1}.

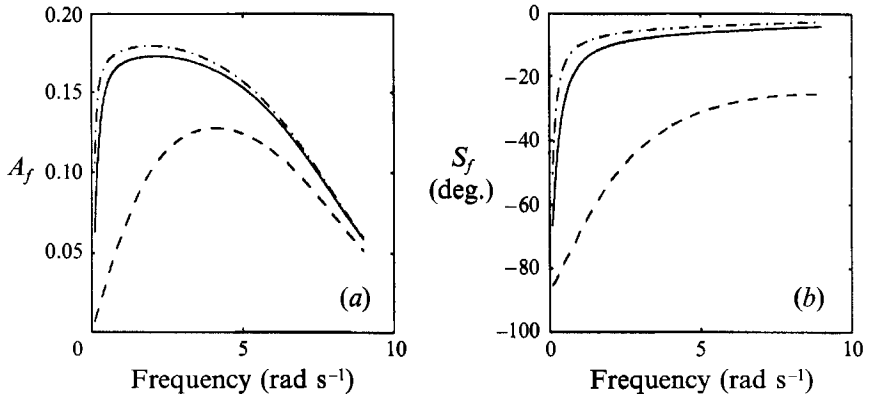

FIGURE 5. (*a*) Amplification factor and (*b*) phase lag. $h_1 = 0.30$ m, $h_2 = 0.09$ m; ν_m(m^2 s^{-1}) = – · –, 5×10^{-4}; —, 10^{-3}; ——, 10^{-2}; $\rho_m = 1230$ Kg m^{-3}.

phase angle shows a change from nearly in-phase motion at intermediate frequency to out of phase for frequencies approaching zero. This phase change is sharper for the smaller viscosity values. This kind of response of the first-order solution could explain the strong variation of the interfacial mass transport velocity that occurs near $\sigma = 1$ rad s^{-1}. For intermediate frequencies, the mass transport seems to be more correlated with both the free surface and interface set-up than with the phase lag.

Finally, figures 6(*a*) and 6(*b*) show the flow rate plotted against the dimensionless wavenumber $K = kh_1$ for various ν_m values. These figures corresponds to the case

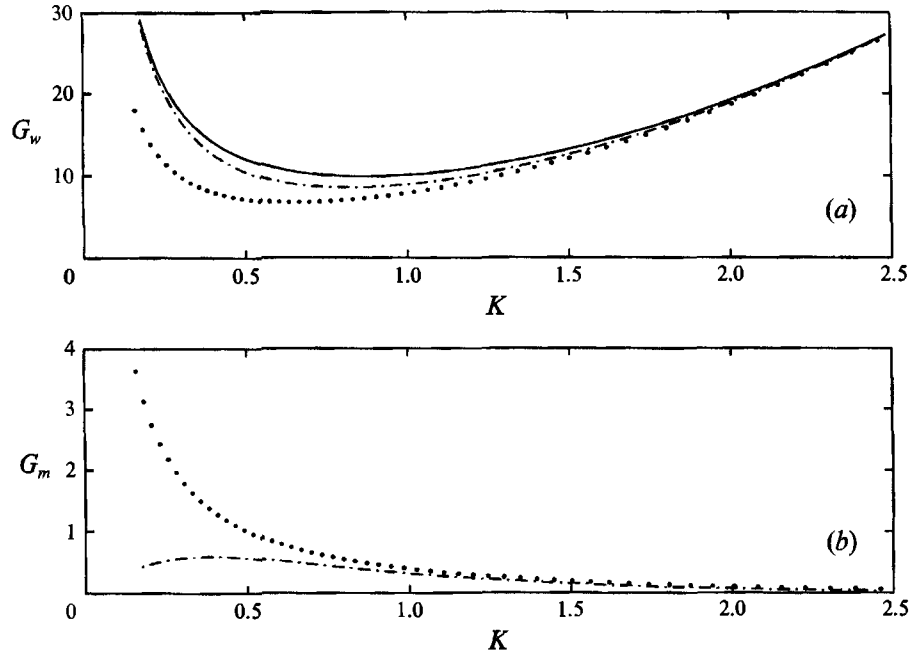

FIGURE 6. Flow rate in an unbounded domain: (*a*) Upper layer, (*b*) lower layer. $h_1 = 0.30$ m, $h_2 = 0.09$ m: —, rigid bed solution; ν_m($m^2\,s^{-1}$) = •, 10^{-4}, – · –, 10^{-2}, $\rho_m = 1230$ Kg m^{-3}.

of waves in an unbounded domain. Figure 6(*a*) correspond to the flow in the upper layer and figure 6(*b*) to the lower layer. The flow rates in both upper and lower layers are obtained by using the stream function defined in (5.5):

$$q_w = -\psi_w(\delta = h_1) + \psi_w(\delta = 0), \qquad q_m = -\psi_m(\delta = 0). \tag{6.26}$$

The dimensionless flow rate G_w and G_m for the upper and lower layers are defined respectively as

$$G_w = 4q_w/(H_s^2\sigma), \quad G_m = 4q_m/(H_s^2\sigma). \tag{6.27}$$

In figure 6(*a*), the solid line represents the flow rate corresponding to the rigid bed solution, given in dimensional form by Ünlüata & Mei (1970) as

$$q = \frac{h_1\sigma H_s^2}{4\sinh^2(kh_1)}\left[\frac{3}{4} + \frac{kh_1}{2}\sinh(2kh_1) + \frac{1}{4kh_1}\sinh(2kh_1)\right]. \tag{6.28}$$

In the lower layer, the flow rate reduces to zero for large K values, as should be expected, since large K means deep water conditions and in this case the bottom is not affected by the surface wave. For small K values, the flow rate increases for deacreasing viscosities.

In the upper layer, it can be seen that for large K values the flow rate approaches the rigid bed solution, since again this case corresponds to deep water conditions. For the range of intermediate K values, the solution approaches the rigid bed solution for the higher viscosity ($\nu_m = 10^{-2}$ $m^2\,s^{-1}$). For the lower viscosity, it can be seen that the sum of the flow rates in the upper and lower layers approaches the rigid bed solution, i.e. the one-layer solution (it should be noted that the rigid bed solution plotted in 6*a* is valid for both h_1 and $h_1 + h_2$).

7. Conclusions

A theoretical model is introduced to determine the mass transport velocity in a two-layer viscous system induced by the action of progressive waves and to study the influence of the properties of the lower layer on the resulting mass transport. The model solves the perturbed form of the mass conservation and momentum equations written in the Lagrangian coordinate system. The solution takes into account wave damping by viscous effects. Comparison with the experiments of Sakakiyama & Bijker (1989) in a water–mud system shows good agreement and an improvement over previous models. The profiles of mass transport velocity measured by these authors are more uniform than those obtained theoretically. The greatest differences appear near the rigid bed. It is thought that this effect is caused by the nonlinearity of the relationship between shear stress and shear rate characteristic of the mud.

The profile of mass transport velocity in both upper and lower layers is obtained analytically for two differents physical situations. The first refers to waves propagating in bounded domains, and the second to waves propagating in unbounded domains, where both the net flux and the set-up can be non-zero.

From this study, the following conclusions can be drawn.

(i) The velocity profiles in both layers are dependent on the wave frequency and on the viscosity of the lower layer. The viscosity of the upper layer was kept constant and equal to the viscosity of water. The velocity at the free surface does not depend on the viscosity of the lower fluid for the larger frequencies (case of bounded domain), but is dependent for smaller ones.

(ii) In the range of frequencies and viscosities studied, the mass transport velocity is smaller than that obtained with the rigid bed solution.

(iii) The interfacial velocity is strongly dependent on both the wave frequency and the viscosity of the lower layer. As found by Dore (1970), the interfacial velocity can be positive (in the direction of wave propagation), but in contrast to Dore's results, it can be negative as well, depending of the lower-layer viscosity.

(iv) For low frequency values, the change of the interfacial velocity seems to be related to the change from almost in phase to out of phase for the free surface motion and the interfacial motion. But for intermediate frequencies it seems more related to the free surface and interface set-up.

(v) In the upper layer, the velocity decreases for decreasing ν_m, while in the lower layer it increases.

(vi) The velocity profile obtained with the condition of zero flux can be completely inverted with respect to the rigid bed solution and its magnitude can be greater at the interface than at the free surface.

(vii) For viscosities lower than 10^{-2} m^2 s^{-1}, the interfacial mass transport shows a complex dependence of both surface wave frequency and viscosity.

(viii) In the bounded domain case, depending on the physical parameters, mass transport in the lower layer can be of the same order of magnitude as in the upper layer (figure 3*d*, $\nu_m=10^{-3}$–10^{-4} m^2 s^{-1}). In the case of unbounded domains, as could occur in real fields, in general the mass transport is in the same direction as the propagation of the surface water wave, and is one order of magnitude higher than in the case of zero flux.

(ix) The high sensitivity of the resulting drift velocity to the lower-layer viscosity should be noted. This suggests that careful studies of the mud rheology should be made before attempting to improve existing models of mass transport in a water–mud system.

The author is grateful to the referees for some helpful suggestions which led to several improvements on an earlier draft of this paper, to Dr Mathieu Mory from LEGI-IMG for his review of this manuscript and his valuable comments and to Professor Julio Borghi from IMFIA for valuable discussions in an initial stage of this work.

Appendix A

$$L_1 = Sl_m L_4 + m_m Sk_2 K_2,\quad L_2 = Cl_m L_4 - Ck_2 K_2,\quad L_3 = m_w(2 - R\,m'). \tag{A 1}$$

$$L_4 = -R\,m' + m_w^2 + 1,\quad m' = m_m^2 + 1,\quad Sk_1 = \sinh kh_1,\quad Ck_1 = \cosh kh_1. \tag{A 2}$$

$$Sk_2 = \sinh kh_2,\quad Ck_2 = \cosh kh_2,\quad Sl_m = \sinh l_m h_2,\quad Cl_m = \cosh l_m h_2. \tag{A 3}$$

$$K_1 = W_4 Sk_1 - W_3 Ck_1,\quad K_2 = 2R - (m_w^2 + 1),\quad g' = g/(\mathrm{i}\sigma v_w k). \tag{A 4}$$

$$K_3 = 2m_w(R - 1),\quad K_4 = -Sl_m/m_m + Sk_2,\quad Clk = -Cl_m + Ck_2. \tag{A 5}$$

$$P_{m1} = \sum_{j_m}\sum_{n_m} H_{j_m n_m}[\cos ah_2 + h_2 \cos ah_2 \Delta_m - \mathrm{e}^{\Delta_m h_2}]. \tag{A 6}$$

$$P_{w1} = -\cos ah_1 A_{w2} + D_{w2} h_1 \sin ah_1 - \sum_{j_w}\sum_{n_w} H_{j_w n_w} \mathrm{e}^{-\Delta_w h_1}. \tag{A 7}$$

$$\begin{aligned} P_{21} = {} & P_{w1} a \cos ah_1/(\sin ah_1) - \sin ah_1 A_{w2} + D_{w2}(\sin ah_1 + ah_1 \cos ah_1) \\ & - \sum_{j_w}\sum_{n_w} H_{j_w n_w} \Delta_w e^{-\Delta_w h_1} - a \sin ah_2 A_{m2} + P_{m1} \frac{\sin ah_2 + ah_2 \cos ah_2}{h_2 \sin ah_2} \\ & + \sum_{j_m}\sum_{n_m} H_{j_m n_m} \Delta_m[-\cos ah_2 + ah_2 \sin ah_2 + \mathrm{e}^{\Delta_m h_2}]. \end{aligned} \tag{A 8}$$

$$\begin{aligned} P_3 = {} & (\hat{T}_m - \rho' v' \hat{T}_w) - \rho' v'[-a^2 P_{w1} - A_{w2} a^2 \cos ah_1 \\ & + D_{w2}(2a \cos ah_1 - a^2 h_1 \sin ah_1) + \sum_{j_w}\sum_{n_w} H_{j_w n_w} \Delta_w^2 \mathrm{e}^{-\Delta_w h_1}] \\ & - A_{m2} a^2 \cos ah_2 + P_{m1}(2a \cos ah_2 - a^2 h_2 \sin ah_2)/(h_2 \sin ah_2) \\ & + \sum_{j_m}\sum_{n_m} H_{j_m n_m} \Delta_m[a^2 h_2 \cos ah_2 + 2a \sin ah_2 + \Delta_m \mathrm{e}^{\Delta_m h_2}]. \end{aligned} \tag{A 9}$$

$$\begin{aligned} P_1 = {} & \sum_{j_w}\sum_{n_w} H_{j_w n_w}[-h_1(a^2 - \Delta_w^2)/(2a) \sin ah_1 - \mathrm{e}^{-\Delta_w h_1}] \\ & + B_{w1} h_1 \cos ah_1 + \sum_{j_m}\sum_{n_m} H_{j_m n_m}(-\cos ah_2 - h_2 \cos ah_2 \Delta_m + \mathrm{e}^{\Delta_m h_2}). \end{aligned} \tag{A 10}$$

$$\begin{aligned} P_{22} = {} & \sum_{j_w}\sum_{n_w} H_{j_w n_w}\left[\frac{a^2 - \Delta^2}{2a}(\sin ah_1 + ah_1 \cos ah_1) - \Delta_w \mathrm{e}^{-\Delta_w h_1}\right] \\ & - A_{m2} a \sin ah_2 - B_{w2}(\cos ah_1 - ah_1 \sin ah_1) \\ & + \sum_{j_m}\sum_{nm} H_{j_m n_m} \Delta_m(-\cos ah_2 + ah_2 \sin ah_2 + \mathrm{e}^{\delta_m h_2}). \end{aligned} \tag{A 11}$$

$$P_4 = -\sum_{j_w}\sum_{n_w} H_{j_w n_w} R^{-1}[(a^2 - \Delta_w^2)/(2a)(2a\cos ah_1 - a^2 h_1 \sin ah_1)$$
$$+\Delta_w^2 e^{-\Delta_w h_1}] + R^{-1} B_{w2}(2a \sin ah_1 + a^2 h_1 \cos ah_1) - A_{m2}(R^{-1} - 2)a^2 \cos ah_2$$
$$+(R^{-1}\hat{T}_w - \hat{T}_m) + \sum_{j_m}\sum_{n_m} H_{j_m n_m}\{\Delta_m[-2a \sin ah_2 + (R^{-1} - 2)a^2 h_2 \cos ah_2]$$
$$+[\Delta_m^2 + (R^{-1} - 1)a^2]e^{\Delta_m h_2}\}. \tag{A 12}$$

$$P_5 = \mathscr{Q} - A_{m2}(1 - \rho')/h_2 a^2(2\cos ah_2 - 1) + \sum_{j_m}\sum_{n_m}\{H_{j_m n_m}\Delta_m$$
$$\times[2a^2 \cos ah_2 + 2/h_2 a(1 - \rho')(\sin ah_2 + h_2 a \cos ah_2)] + H_{j_m n_m}\Delta_m^3 e^{\Delta m h_2}$$
$$-(1 - \rho')/h_2[H_{j_m n_m}\Delta_m^2(1 - e^{\Delta m h_2})a^2 H_{j_m n_m} e^{\Delta m h_2}] + a^2 H_{j_m n_m}\Delta_m e^{\Delta m h_2}\}, \tag{A 13}$$

where

$$\mathscr{Q} = \frac{1 - \rho'}{h_2} T_m(h_2) - \frac{1 - \rho'}{\nu_m}\left[\frac{\mathscr{S}_{xx\alpha}}{\rho_m h_2} + \rho' g \xi_{w\alpha}\right] - \frac{(1 - \rho')Q_{mn} + Q_{mv}}{\nu_m}. \tag{A 14}$$

REFERENCES

ANDREWS, D. G. & MCINTRE, M. E. 1978 An exact theory of nonlinear waves on a Lagrangian-mean flow. *J. Fluid Mech.* **89**, 609–645.

BATCHELOR, G. K. 1967 *An Introduction to Fluid Dynamics.* Cambridge University Press.

CHANG, M. S. 1969 Mass transport in deep-water long-crested random gravity waves. *J. Geophys. Res.* **74**, 1515–1537.

CRAIK, A. D. 1982 The drift velocity of water waves. *J. Fluid Mech.* **116**, 187–205.

R. DALRYMPLE & LIU, P. L.-F. 1978 Water waves over soft mud: A two layer fluid model. *J. Phys. Oceanogr.* **8**, 1121–1131.

DORE, B. D. 1970 Mass transport in a layered fluid system. *J. Fluid Mech.* **40**, 113–126.

DORE, B. D. 1973 On mass transport induced by interfacial oscillations at single frequency. *Proc. Camb. Phil. Soc.* **74**, 333–347.

FODA, M. A., HUNT, J. R. & CHOU, H.-T. 1993 A non-linear model for the fluidization of marine mud by waves. *J. Geophys. Res.* **98**, 7039–7047.

GRIMSHAW, R. 1981 Mean flows generated by a progressing water wave packet. *J. Austral. Math. Society.* B **22**, 318–347.

HUANG, N. E. 1970 Mass transport induced by wave motion. *J. Mar. Res.* **28**, 35–50.

HUNT, J. N. 1964 The viscous damping of gravity waves in shallow water. *La Houille Blanche* **6**, 685–691.

ISKANDARANI, M. & LIU, P. L.-F. 1991 Mass transport in two-dimensional water waves. *J. Fluid Mech.* **231**, 395–415.

KRAVTCHENKO, J. & DAUBERT, A. 1957 La houle a trajectoires fermés en profondeur fini. *La Houille Blanche* **3**, 408–429.

LONGUET-HIGGINS, M. S. 1953 Mass transport in water waves. *Phil. Trans. R. Soc. Lond.* A **67**, 535–581.

MEI, C. C. 1989 *The Applied Dynamics of Ocean Surface Waves.* World Scientific.

MICHE, M. 1944 Mouvements ondulatoires de la mer en profondeur constante ou decroissent. *Ann. Ponts Chaussees*, 25–78.

MIGNIOT, C. 1968 Etude des propiétés physiques de différents sédiments trés fins et de leurs comportement sous des actions hydrodinamiques. *La Houille Blanche* **7**, 591–620.

PIEDRA-CUEVA, I. 1993 On the response of a muddy bottom to surface water waves. *J. Hydraul. Res.* **31**, 681–697.

PIERSON, W. J. 1962 Perturbation analysis of the Navier-Stokes equation in Lagrangian form with selected linear solutions. *J. Geophys. Res.* **67**, 3151–3160.

SAKAKIYAMA, T. & BIJKER, E. 1989 Mass transport velocity in a mud layer due to progressive waves. *J. Port, Coastal Ocean Engng* **115**, 614–632.

SHIBAYAMA, T., TAKIKAWA, H. & HORIKAWA, K. 1986 Mud mass transport due to waves. *Coastal Engng Japan* **29**, 151–161.

SWAN, C. & SLEATH, J. F. A. 1990 A second approximation to the time-mean Lagrangian drift beneath a series of progressive gravity waves. *Ocean Engng* **17**, 65–79.

TSURUYA, H., NAKANO, S. & TAKAHAMA, J. 1987 Interactions between surface waves and a multi-layered mud bed. *Rep. Port Harbour Res. Inst. (Japan)* **26** (5), 137–173.

ÜNLÜATA, U. & MEI, C. C. 1970 Mass transport in water waves. *J. Geophys. Res.* **75**, 7611–7618.